

Mathematical and Statistical Process Modeling of Hydrochloric Acid Leaching of Iron-Oxide Impurity from Inyi Kaolin: Response Surface Methodology

John Sunday Uzochukwu^{1*}, Onu Chijioke Elijah², Ohale Pascal Enyinnaya³, N. Nweke Chinenye⁴,
Madiebo Emeka Michael⁵, John Chioma Mary⁶

^{1,2,3,4,5,6}Department of Chemical Engineering, Nnamdi Azikiwe University, Awka, Nigeria

Abstract: The iron-oxide impurity is comparatively abundant in the low-grade kaolin from Inyi in Enugu, Nigeria. The iron-oxide impurities in kaolin make it unsuitable for industrial use. This study focused on the mathematical and statistical process modeling of iron-oxide impurity leaching from Inyi Kaolin by hydrochloric acid (HCl). Response Surface Methodology (RSM) was used to examine the combined effects of leaching temperature, solid-liquid ratio, reaction time, stirring speed, particle size, and acid concentration on the removal of iron contaminant from the local kaolin in HCl. The second-order polynomial regression equation designed with a correlation coefficient R^2 of 0.9959 provided the best description for the experimental data. The leaching temperature of 79.99°C, the solid-liquid ratio of 0.021, and the reaction time of the leaching temperature was 79.99°C, the solid-liquid ratio was 0.021, the reaction duration was 240 minutes, the stirring speed was 580.985 rpm, the particle size was 0.045mm, the acid concentration was 3.513mol/cm³, and the yield was at its highest point of 94.35%.

Keywords: Kaolin, leaching, iron-oxide impurity, hydrochloric acid, ANOVA, process modeling.

1. Introduction

Kaolin is a natural resource utilized in industrial applications counting ceramics, paper, paints, fiberglass, printing inks, pharmaceuticals, cement, etc. (Murray and Keller, 1993; Ajana et al., 2015; Nnanwube et al., 2018). The proximity of impurities, especially materials containing titanium and iron, gives kaolin its color. In the process of weathering or hydrothermal changes, significant amounts of iron oxides can accumulate, making the compacted kaolin clay unsuitable for industrial use (Martínez-Luévanos et al., 2011; Ajana et al., 2015).

Hence, a few chemical strategies have been utilized to improve kaolin to diminish these impurities (Lee et al., 2006, 2007; Martínez-Luévanos et al., 2011; Ambikadevi and Lalithambika, 2000; Ajana et al., 2015; Veglio et al., 1996; Nnanwube et al., 2018). The leaching of iron oxide from kaolin is of uncommon intrigue to makers of industrial minerals like kaolin. The leaching operation is one of the most important

process steps in the hydrometallurgical industrial operation and processing of kaolin for commercial application.

The kinetic, mathematical, and statistical process modeling of the reaction mechanism and the process variables which impact the hydrometallurgical process is very vital in the process and plant development and design.

The leaching kinetics of iron oxides in oxalic acid and oxalate solutions has been significantly published (Blesa et al., 1987; 1994; Panias et al., 1996; Veglio and Toro, 1993; Ajana et al., 2015; Nnanwube et al., 2018). The removal prospects of iron oxide by acid washing have been reported (Lee et al., 2006). Ambikadevi and Lalithambika (2000) reported the leaching efficiency of iron from clay using some organic acids as dissolution solvents. The efficiency of this operation in the removal of iron impurities is extremely significant for process and plant design. The efficiency of the dissolution process is dependent on operating conditions including the clay type, concentration of acid, acid/clay ratio, dissolution reaction time, and temperature (Lui et al, 2010; Ajana et al., 2015; Abali et al, 2006; Nnanwube et al., 2018). The leaching temperature, liquid-solid ratio, calcination temperature, acid concentration, and stirring speed have been reported as very significant process variables that influence the leaching operation (Ozdemir and Cetisli, 2005; Eisele, 1983; Al-Zahrani and Abdul, 2009; Ajana et al., 2015; Poppleton and Sawyer, 1977; Nnanwube et al., 2018).

The traditional and conservative methods of examining a process by one factor at a time sequence do not account for the combined effect of the entire process variables entailed (Kumar, Prasad, and Mishra, 2008). This strategy is laborious, tedious, and expensive and demands a large-scale experimental investigation for the determination of unreliable optimum operating conditions. These drawbacks can be solved by optimization of the leaching operation parameters together with mathematical and statistical experimental design such as response surface methodology (Ajana et al., 2015; Ko, Porter, and Mckay, 2000; Nnanwube et al., 2018).

*Corresponding author: su.john@unizik.edu.ng

Response surface methodology is founded on polynomial surface analysis which is a compendium of mathematical and statistical techniques valuable for the analysis and modeling of problems with a process response of intrigue affected by some variables (Park and Ahn, 2004). The hallmark of response surface methodology is focused on the determination of the optimum process conditions for the operation (Kumar *et al.*, 2008; Ajana *et al.*, 2015; Nnanwube *et al.*, 2018). The statistical experimental design techniques applied in leaching process development and design enhance the product yields, close up the output response to target obligations, reduce operational variability, and conserve time and total costs (Annadurai, Juang, and Lee, 2002; Ajana *et al.*, 2015; Nnanwube *et al.*, 2018). In this work, the optimum process conditions for the leaching of iron-oxide impurity from Inyi kaolin in hydrochloric acid are studied by applying the central composite design of the response surface methodology.

2. Materials and Methods

A sample of Inyi kaolin was mined at the quarry and separated from the contaminated debris. The mined kaolin samples were sun-dried for 3 days and were then ground in a mortar and sieved through a 75 μm sieve. The selected samples were then calcined in a furnace. Firing temperatures were chosen in the range of 400 $^{\circ}\text{C}$ to 850 $^{\circ}\text{C}$ for all samples. Firing times also varied from 0.3 hours to 6 hours.

A. Dissolution Experiment

The calcined samples were ground and sieved into different particle sizes and labeled in like manner. For each test, 1g of the measured divisions was weighed out and reacted with 100 ml of the acids in a 250 ml bottomed flask. The jar and its substance were heated to a fixed temperature of 90 $^{\circ}\text{C}$ on a magnetic blending plate and blending was proceeded all through the reaction length. Too, the reactor was fitted with a reflux condenser to anticipate misfortunes by vanishing. After the reaction time was completed, the suspension was promptly sifted to isolate un-dissolved materials and washed three times with distilled water. The resulting solutions were diluted and analyzed for iron oxides utilizing MS Atomic Absorption Spectrophotometer. The buildup was too collected, washed to lack of bias with distilled water, air dried, and oven dried at 60 $^{\circ}\text{C}$, and after that reweighed. The distinction in weight was noted for deciding the fraction of the iron oxide that dissolved.

B. Design of Experiment

RSM was used in conjunction with a five-level, six-factor fractional factorial design created by Design Expert software (9.0.1 trial version) to study the leaching process factors

impacting the iron oxide removal from the Inyi kaolin sample in hydrochloric acid. The reaction temperature ranged from 50 to 900C, the acid concentration ranged from 1 to 7mol/l, the solid-to-liquid ratio ranged from 0.02 to 0.10g/ml, the stirring speed ranged from 180 to 900rpm, the particle size ranged from 0.045 to 0.212MM, and the reaction time ranged from 30 to 240 minutes. Iron impurity conversion percentage was used as the response variable. The levels of the factors were labeled as - α , - 1, 0, +1, and + α . Table 1 displays the levels and the range. To optimize the process variables, 86 runs were done, and experiments were carried out per the actual experimental design matrix provided in Table 2. To avoid a systemic error, the experiments were carried out at random. The coefficient of determination, analysis of variance (ANOVA), and response plots were used to examine the results. The second-order polynomial equation created to fit the experimental data and identify the important model terms is given in the following sequence in RSM:

$$Y = \beta_0 + \sum \beta_i x_i + \sum \beta_{ii} x_{ii}^2 + \sum \beta_{ij} x_i x_j + \epsilon \quad (1)$$

Where Y is the expected response variable, in this case, the percentage of iron oxide removed, β_0 is the constant coefficient, β_i is the input variable's i^{th} linear coefficient, β_{ii} is the input variable's i^{th} quadratic coefficient, β_{ij} is the various interaction coefficients between the input variables x_i and x_j , and is the model's error.

3. Results and Discussion

The combined impact of process parameters on the test iron extraction efficiency was explored. The removal efficiency of iron debasements from kaolin progressed with expanding dissolution temperature, concentration, reaction time, and mixing speed. The experimental result of the combined impact of the process factors on the response (removal of iron debasements) is displayed in Table 2.

A. Model Generation

The data produced from the experiments (Table 3) were measurably analyzed to distinguish the critical primary intuitive and quadratic impacts. The multi-regression examination was performed on the data to get a quadratic response surface model for the leaching of iron debasement from the kaolin. The ultimate second-order (quadratic model) polynomial prescient equation gotten for the examination of iron leaching with HCl from Inyi kaolin is displayed in equation (2) as taken after:

Table 1
Experimental range of the independent variables, with different levels, to study iron oxide removal during the dissolution of Inyi kaolin in hydrochloric acid

Independent variables	Symbols	Range and levels				
		- α	-1	0	+1	+ α
Leaching temp. ($^{\circ}\text{C}$)	X_1	38.70	50	70	90	101.3
Acid conc. (mol/cm 3)	X_2	0.70	1	4	7	8.70
Particle size (mm)	X_3	0.06	0.0408	0.23	0.41	0.51
Stirring speed (rpm)	X_4	23.43	180	540	900	1103.43
Solid/Liquid ratio (g/cm 3)	X_5	0.01	0.02	0.60	1	0.12
Time (mins)	X_6	5.33	30	135	240	299.33

Table 2
Experimental design/plan for iron oxides impurity removal from Inyi kaolin sample

Std	Leaching temp (°C) X ₁		Acid conc. (M) X ₂		Part.size (mm) X ₃		Stirring speed (rpm) X ₄		Solid/liquid ratio (g/ml) X ₅		Time (mins) X ₆		Response
	Coded	Real	Coded	Real	Coded	Real	Coded	Real	Coded	Real	Coded	Real	Efficiency(%)
1	-1	50	-1	1	-1	0.04	-1	180	-1	0.02	-1	30	74.24
2	1	90	-1	1	-1	0.04	-1	180	-1	0.02	-1	30	74.24
3	-1	50	1	7	-1	0.04	-1	180	-1	0.02	-1	30	52.32
4	1	90	1	7	-1	0.04	-1	180	-1	0.02	-1	30	66
5	-1	50	-1	1	1	0.41	-1	180	-1	0.02	-1	30	46.72
6	1	90	-1	1	1	0.41	-1	180	-1	0.02	-1	30	74.24
7	-1	50	1	7	1	0.41	-1	180	-1	0.02	-1	30	50.22
8	1	90	1	7	1	0.41	-1	180	-1	0.02	-1	30	12.28
9	-1	50	-1	1	-1	0.04	1	900	-1	0.02	-1	30	51.16
10	1	90	-1	1	-1	0.04	1	900	-1	0.02	-1	30	12.28
11	-1	50	1	7	-1	0.04	1	900	-1	0.02	-1	30	50.22
12	1	90	1	7	-1	0.04	1	900	-1	0.02	-1	30	66
13	-1	50	-1	1	1	0.41	1	900	-1	0.02	-1	30	10.84
14	1	90	-1	1	1	0.41	1	900	-1	0.02	-1	30	50.22
15	-1	50	1	7	1	0.41	1	900	-1	0.02	-1	30	12.28
16	1	90	1	7	1	0.41	1	900	-1	0.02	-1	30	66
17	-1	50	-1	1	-1	0.04	-1	180	1	0.1	-1	30	10.84
18	1	90	-1	1	-1	0.04	-1	180	1	0.1	-1	30	66
19	-1	50	1	7	-1	0.04	-1	180	1	0.1	-1	30	50.82
20	1	90	1	7	-1	0.04	-1	180	1	0.1	-1	30	50.22
21	-1	50	-1	1	1	0.41	-1	180	1	0.1	-1	30	11.64
22	1	90	-1	1	1	0.41	-1	180	1	0.1	-1	30	74.24
23	-1	50	1	7	1	0.41	-1	180	1	0.1	-1	30	66
24	1	90	1	7	1	0.41	-1	180	1	0.1	-1	30	66
25	-1	50	-1	1	-1	0.04	1	900	1	0.1	-1	30	74.24
26	1	90	-1	1	-1	0.04	1	900	1	0.1	-1	30	66
27	-1	50	1	7	-1	0.04	1	900	1	0.1	-1	30	11.84
28	1	90	1	7	-1	0.04	1	900	1	0.1	-1	30	51.62
29	-1	50	-1	1	1	0.41	1	900	1	0.1	-1	30	10.84
30	1	90	-1	1	1	0.41	1	900	1	0.1	-1	30	66
31	-1	50	1	7	1	0.41	1	900	1	0.1	-1	30	12.28
32	1	90	1	7	1	0.41	1	900	1	0.1	-1	30	66
33	-1	50	-1	1	-1	0.04	-1	180	-1	0.02	1	240	74.24
34	1	90	-1	1	-1	0.04	-1	180	-1	0.02	1	240	11.84
35	-1	50	1	7	-1	0.04	-1	180	-1	0.02	1	240	74.22
36	1	90	1	7	-1	0.04	-1	180	-1	0.02	1	240	12.28
37	-1	50	-1	1	1	0.41	-1	180	-1	0.02	1	240	50.22
38	1	90	-1	1	1	0.41	-1	180	-1	0.02	1	240	10.84
39	-1	50	1	7	1	0.41	-1	180	-1	0.02	1	240	66
40	1	90	1	7	1	0.41	-1	180	-1	0.02	1	240	12.28
41	-1	50	-1	1	-1	0.04	1	900	-1	0.02	1	240	74.24
42	1	90	-1	1	-1	0.04	1	900	-1	0.02	1	240	49.82
43	-1	50	1	7	-1	0.04	1	900	-1	0.02	1	240	10.84
44	1	90	1	7	-1	0.04	1	900	-1	0.02	1	240	66
45	-1	50	-1	1	1	0.41	1	900	-1	0.02	1	240	10.84
46	1	90	-1	1	1	0.41	1	900	-1	0.02	1	240	50.3
47	-1	50	1	7	1	0.41	1	900	-1	0.02	1	240	74.24
48	1	90	1	7	1	0.41	1	900	-1	0.02	1	240	10.84
49	-1	50	-1	1	-1	0.04	-1	180	1	0.1	1	240	23.28
50	1	90	-1	1	-1	0.04	-1	180	1	0.1	1	240	74.24
51	-1	50	1	7	-1	0.04	-1	180	1	0.1	1	240	74.24
52	1	90	1	7	-1	0.04	-1	180	1	0.1	1	240	12.28
53	-1	50	-1	1	1	0.41	-1	180	1	0.1	1	240	10.84
54	1	90	-1	1	1	0.41	-1	180	1	0.1	1	240	50.22
55	-1	50	1	7	1	0.41	-1	180	1	0.1	1	240	12.28
56	1	90	1	7	1	0.41	-1	180	1	0.1	1	240	12.28
57	-1	50	-1	1	-1	0.04	1	900	1	0.1	1	240	45.3
58	1	90	-1	1	-1	0.04	1	900	1	0.1	1	240	10.84
59	-1	50	1	7	-1	0.04	1	900	1	0.1	1	240	73
60	1	90	1	7	-1	0.04	1	900	1	0.1	1	240	12.28
61	-1	50	-1	1	1	0.41	1	900	1	0.1	1	240	10.84
62	1	90	-1	1	1	0.41	1	900	1	0.1	1	240	12.28
63	-1	50	1	7	1	0.41	1	900	1	0.1	1	240	66
64	1	90	1	7	1	0.41	1	900	1	0.1	1	240	10.84
65	-1.56	38.7	0	4	0	0.23	0	540	0	0.06	0	135	12.28

66	1.56	101.3	0	4	0	0.23	0	540	0	0.06	0	135	66
67	0	70	-1.56	-0.7	0	0.23	0	540	0	0.06	0	135	74.24
68	0	70	1.56	8.7	0	0.23	0	540	0	0.06	0	135	66
69	0	70	0	4	-1.56	0.06	0	540	0	0.06	0	135	12.28
70	0	70	0	4	1.56	0.51	0	540	0	0.06	0	135	74.24
71	0	70	0	4	0	0.23	-1.56	30	0	0.06	0	135	50.32
72	0	70	0	4	0	0.23	1.56	1103	0	0.06	0	135	74.24
73	0	70	0	4	0	0.23	0	540	-1.56	0.02	0	135	50.22
74	0	70	0	4	0	0.23	0	540	1.56	0.12	0	135	66
75	0	70	0	4	0	0.23	0	540	0	0.06	-1.56	30	10.84
76	0	70	0	4	0	0.23	0	540	0	0.06	1.56	299.33	74.24
77	0	70	0	4	0	0.23	0	540	0	0.06	0	135	50.22
78	0	70	0	4	0	0.23	0	540	0	0.06	0	135	66
79	0	70	0	4	0	0.23	0	540	0	0.06	0	135	74.24
80	0	70	0	4	0	0.23	0	540	0	0.06	0	135	10.84
81	0	70	0	4	0	0.23	0	540	0	0.06	0	135	50.22
82	0	70	0	4	0	0.23	0	540	0	0.06	0	135	50.12
83	0	70	0	4	0	0.23	0	540	0	0.06	0	135	47.32
84	0	70	0	4	0	0.23	0	540	0	0.06	0	135	10.84
85	0	70	0	4	0	0.23	0	540	0	0.06	0	135	12.28
86	0	70	0	4	0	0.23	0	540	0	0.06	0	135	12.28

Table 3
Sequential model sum of squares and the model summary statistics

Source	Sum of Squares	Df	Mean Square	F Value	p-value	Prob > F	Remark
Mean vs Total	1.576E+005	1	1.576E+005				
Linear vs Mean	56180.21	6	9363.37	423.72	< 0.0001		
2FI vs Linear	194.62	15	12.97	0.54	0.9107		
Quadratic vs 2FI	1436.69	6	239.45	121.38	< 0.0001		Suggested
Cubic vs Quadratic	45.65	27	1.69	0.76	0.7617		Aliased
Residual	68.77	31	2.22				
Total	2.155E+005	86	2506.25				

Lack of Fit Tests							
Source	Sum of Squares	Df	Mean Square	F Value	p-value	Prob > F	Remark
Linear	1718.84	70	24.55	8.22	0.0010		
2FI	1524.22	55	27.71	9.28	0.0006		
Quadratic	87.53	49	1.79	0.60	0.8786		Suggested
Cubic	41.88	22	1.90	0.64	0.8140		Aliased
Pure Error	26.89	9	2.99				

Model Summary Statistics						
Source	Std. Dev.	R-Squared	Adjusted R-Squared	Predicted R-Squared	PRESS	Remark
Linear	4.70	0.9699	0.9676	0.9664	1945.14	
2FI	4.92	0.9732	0.9644	0.9649	2035.28	
Quadratic	1.40	0.9980	0.9971	0.9959	236.46	Suggested
Cubic	1.49	0.9988	0.9967		+	Aliased

$$\%Y_{\text{Iron oxide impurity}} = 49.5828 + 2.46958 * X_1 + -0.127419 * X_2 + 0.172775 * X_3 + -0.133068 * X_4 + 0.129379 * X_5 + 29.0678 * X_6 + -0.171563 * X_1X_2 + 0.203437 * X_1X_3 + -0.157812 * X_1X_4 + 0.247813 * X_1X_5 + 1.60406 * X_1X_6 + -0.172187 * X_2X_3 + 0.126562 * X_2X_4 + -0.216563 * X_2X_5 + 0.127187 * X_2X_6 + -0.248437 * X_3X_4 + 0.158438 * X_3X_5 + -0.185312 * X_3X_6 + -0.202812 * X_4X_5 + 0.140938 * X_4X_6 + -0.140937 * X_5X_6 + -0.639514 * X_1^2 + 0.267767 * X_2^2 + 0.155483 * X_3^2 + 0.201958 * X_4^2 + 0.179423 * X_5^2 + -9.03324 * X_6^2 \tag{2}$$

The adequacy of the model was tested using the sequential model sum of squares and the model summary statistics (Table 3). At 0.05 level of significance, only the quadratic model is significant which gave the regression coefficient of 0.9980 showing that the model adequately explained 99.80% of the variation and also, the R² adjusted of 0.9971 is in reasonable agreement with the R² predicted of 0.9959 for the quadratic model.

The evaluation of variance (NOVA) was offered in Table 4. The P values have been used as a tool to test the importance of the individual coefficients, which in flip are vital to apprehend the pattern of the mutual interactions among the check variables

(Shrivastava, Saudagar, Bajaj, and Singhal, 2008). The bigger the value of the F-test price and the smaller the magnitude of the P-values, the higher the significance of the corresponding coefficient (Alam, Muyibi, Kamaldin, 2008). Values of P less than 0.05 imply that the version phrases are widespread. The very last mathematical version by way of eliminating the pale terms and interactions is expressed in equation (3).

$$\%Y_{\text{IRON OXIDE IMPURITY}} = 49.5828 + 2.46958 * X_1 + 29.0678 * X_6 + 1.60406 * X_1X_6 + -9.03324 * X_6^2 \tag{3}$$

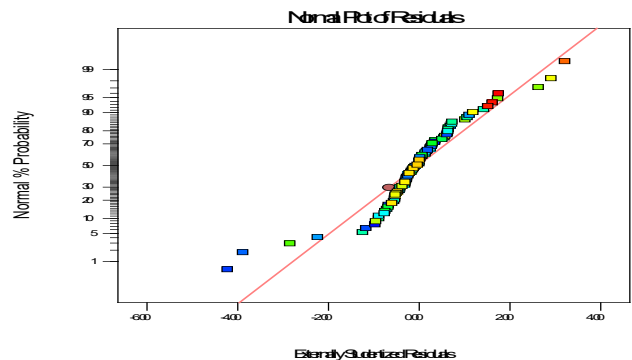


Fig. 1. Plot of normal probability versus residuals

Table 4
ANOVA and regression analysis for the Response Surface Quadratic model

Analysis of variance table [Partial sum of squares - Type III]						
Source	Sum of Squares	df	Mean Square	F Value	p-value Prob > F	Remark
Model	57811.52	27	2141.17	1085.37	< 0.0001	Significant
X1-temp	420.20	1	420.20	213.00	< 0.0001	
X2-conc	1.09	1	1.09	0.55	0.4608	
X3-particle size	1.98	1	1.98	1.00	0.3209	
X4-stirring speed	1.21	1	1.21	0.61	0.4364	
X5-solid/liquid ratio	1.15	1	1.15	0.58	0.4491	
X6-time	56234.79	1	56234.79	28505.73	< 0.0001	
X1X2	1.88	1	1.88	0.95	0.3325	
X1X3	2.65	1	2.65	1.34	0.2513	
X1X4	1.59	1	1.59	0.81	0.3724	
X1X5	3.93	1	3.93	1.99	0.1634	
X1X6	164.67	1	164.67	83.47	< 0.0001	
X2X3	1.90	1	1.90	0.96	0.3308	
X2X4	1.03	1	1.03	0.52	0.4739	
X2X5	3.00	1	3.00	1.52	0.2224	
X2X6	1.04	1	1.04	0.52	0.4717	
X3X4	3.95	1	3.95	2.00	0.1624	
X3X5	1.61	1	1.61	0.81	0.3706	
X3X6	2.20	1	2.20	1.11	0.2956	
X4X5	2.63	1	2.63	1.33	0.2528	
X4X6	1.27	1	1.27	0.64	0.4254	
X5X6	1.27	1	1.27	0.64	0.4254	
X1^2	5.35	1	5.35	2.71	0.1051	
X2^2	0.64	1	0.64	0.32	0.5710	
X3^2	0.20	1	0.20	0.10	0.7512	
X4^2	0.47	1	0.47	0.24	0.6283	
X5^2	0.37	1	0.37	0.19	0.6670	
X6^2	696.02	1	696.02	352.82	< 0.0001	
Residual	114.42	58	1.97			not significant
Lack of Fit	87.53	49	1.79	0.60	0.8786	
Pure Error	26.89	9	2.99			
Cor Total	57925.94	85				
Std. Dev.	1.40		R-Squared		0.9980	
Mean	42.81		Adj R-Squared		0.9971	
C.V. %	3.28		Pred R-Squared		0.9959	
PRESS	236.46		Adeq Precision		81.761	

Advance approval of the quadratic model was done with the typical likelihood of residuals plot (Fig. 1) and plot of anticipated versus real (Fig. 2). The residuals can be judged as regularly dispersed; in this manner, typicality presumptions of the response is fulfilled.

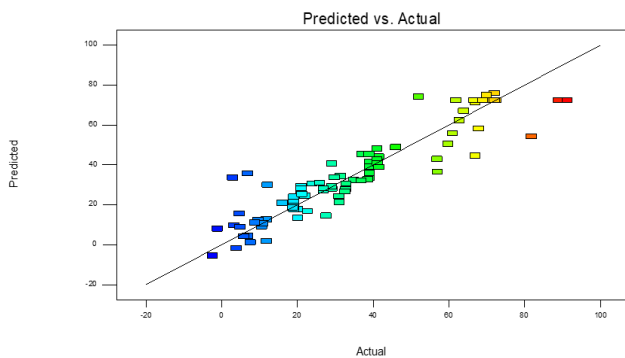


Fig. 2. Plot predicted values versus actual values

B. Response Surface Plots of Iron Dissolution in HCL

The intelligent impacts of the process factors on the rate of iron removal were examined by plotting three-dimensional surface bends against any two free factors whereas keeping other variables at their central (0) level. The 3D bends of the response (rate removal) and form plots from the intelligence between the factors are shown in Figures 3 – 17.

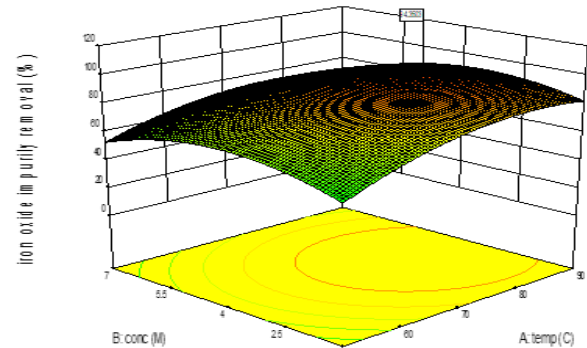


Fig. 3. 3D plot of the effect of acid conc. and temp on % iron impurity removal

The interactive impact of process temperature (Figures 3, 4, 5, 6, and 7) appeared that an increment in temperature expanded the yield of iron oxide impurity for up to around 79.99°C, and advance increment had no critical enhancement in iron contaminant removal. The intelligent impact of acid concentration (Figures 3, 8, 9, 10, and 11) uncovered that iron disintegration expanded as the acid concentration expanded. Optimum iron debasement removal was gotten at around an acid concentration of 3.513mol/cm³, and advance increment had no noteworthy change in iron debasement removal. The intelligent impact of the kaolin-acid proportion (Figures 6, 10, 13, 15, and 17) showed diminished iron impurity removal with

the increment within the kaolin-acid proportion. The optimum result was accomplished with a proportion of 0.021. The intuitive impact of mixing speed (Figures 5, 9, 12, 15, and 16) uncovered an increment in iron impurity removal with blending speed up to the optimum value of 580.985rpm and advance increment had no critical advancement on iron debasement removal.

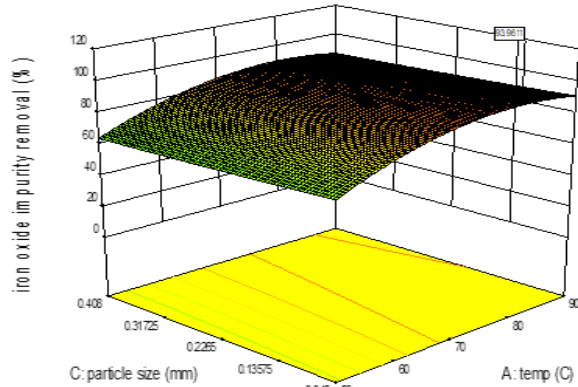


Fig. 4. 3D plot of the effect of part. size and temp. on % iron impurity removal

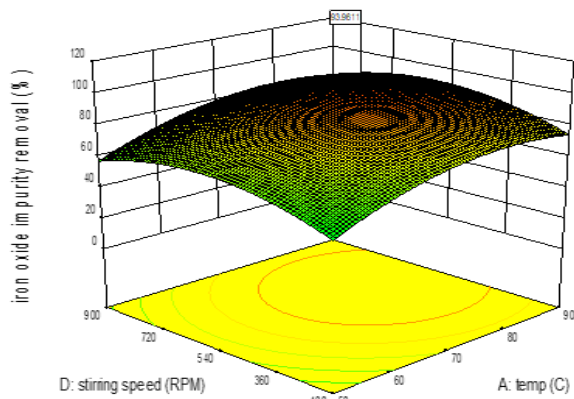


Fig. 5. 3D plot of the effect of stirring speed and temp. on % iron impurity removal

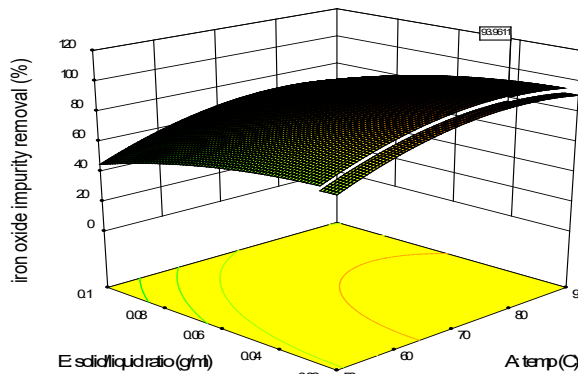


Fig. 6. 3D plot of the effect of solid/liquid ratio and temp. on % iron impurity removal

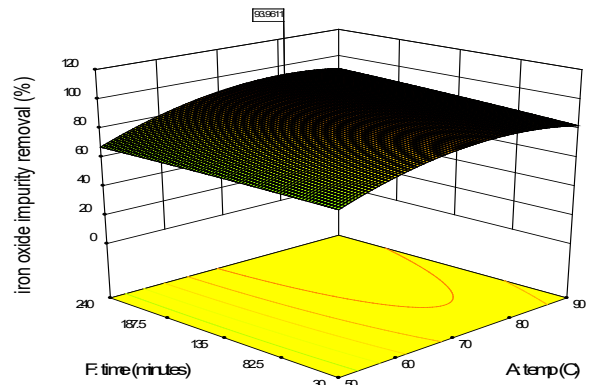


Fig. 7. 3D plot of the effect of time and temp. on % iron impurity removal

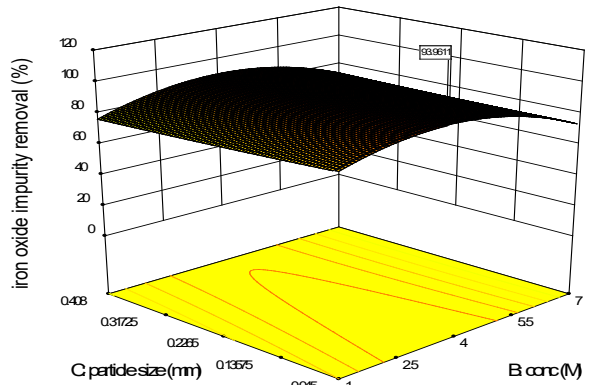


Fig. 8. 3D plot of the effect of particle size and conc. on % iron impurity removal

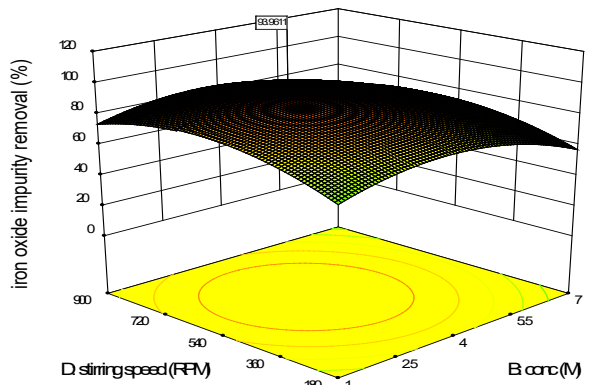


Fig. 9. 3D plot of the effect of stirring speed and conc. on % iron impurity removal

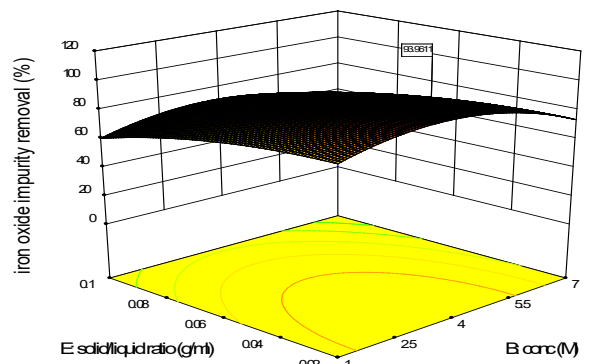


Fig. 10. 3D plot of the effect of solid/liquid ratio and conc. on % iron impurity removal

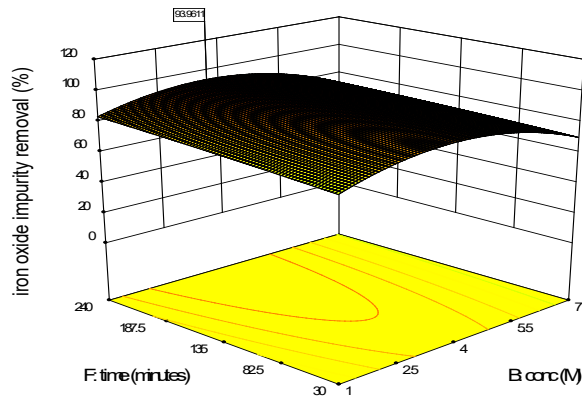


Fig. 11. 3D plot of the effect of time and conc. on % iron impurity removal

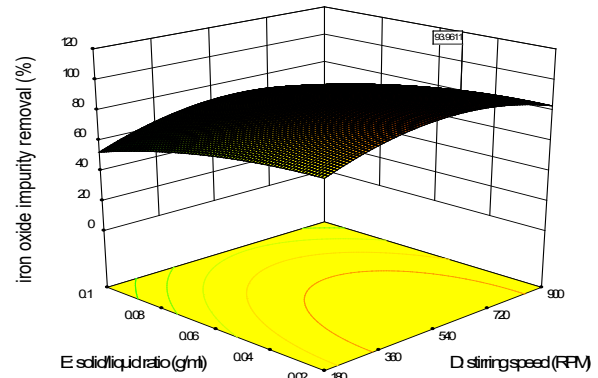


Fig. 15. 3D plot of the effect of solid/liquid ratio and stirring speed on % iron impurity

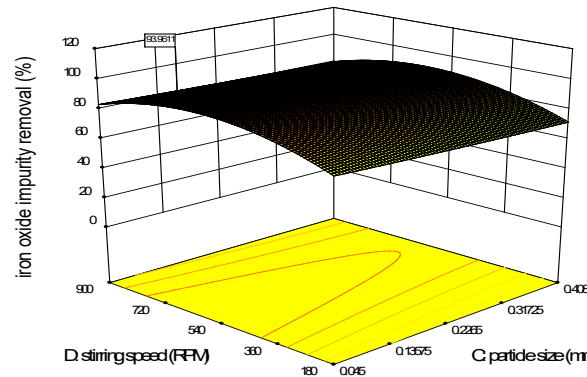


Fig. 12. 3D plot of the effect of stirring speed and particle size on % iron impurity

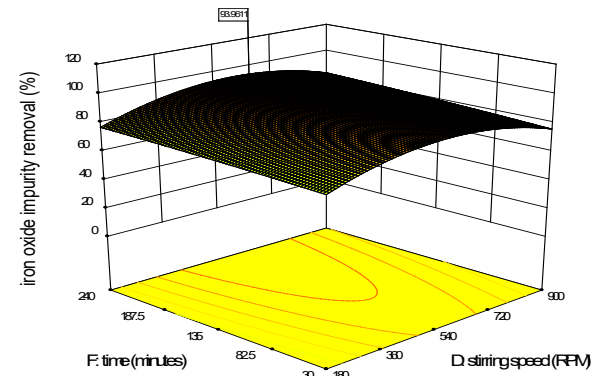


Fig. 16. 3D plot of the effect of time and stirring speed on % iron impurity removal

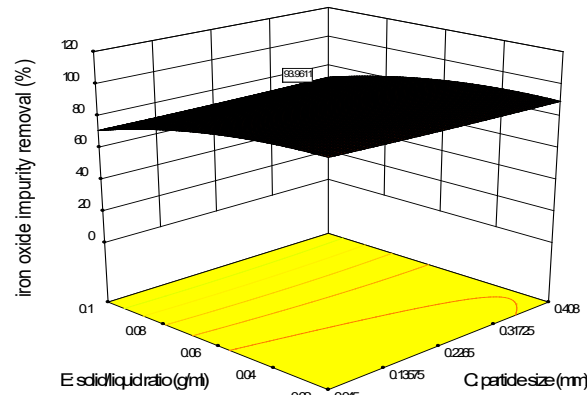


Fig. 13. 3D plot of the effect of solid/liquid ratio and part. size on % iron impurity

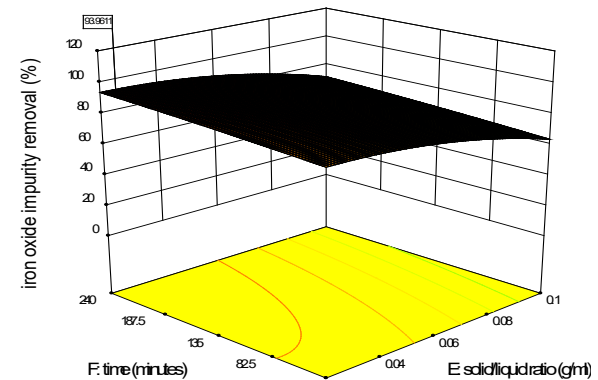


Fig. 17. 3D plot of the effect of time and solid/liquid ratio on % iron impurity removal

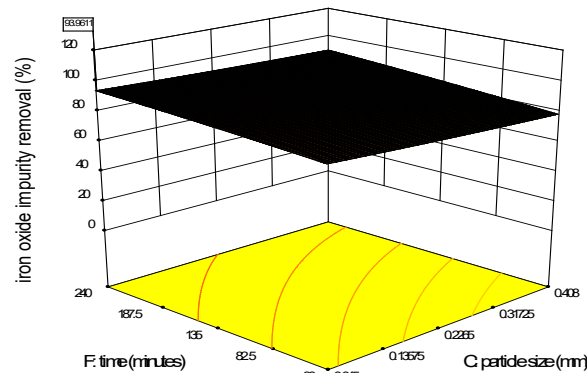


Fig. 14. 3D plot of the effect of time and part. size on % iron impurity removal

C. Numerical Optimization and Validation of Optimization Result

The following conditions were predicted to yield 93.987% in the dissolution of iron with HCl from Inyi kaolin: leaching temperature of 79.99°C; acid concentration of 3.513mol/cm³; solid/liquid ratio of 0.021g/ml, particle size of 0.045mm, stirring speed of 580.985rpm, and reaction time of 240 minutes. The optimization was carried out utilizing the numerical method of State Ease U.S.A.'s Design Expert version 9.0. The result is quite close to the experimental value of 94.32% obtained at the same optimum process variable values.

4. Conclusion

The influence of important parameters on the % iron output

was examined using response surface methods. The Box Wilson design was utilized to optimize the process. Based on the findings of this study, it is possible to achieve a yield of 94.32% under the ideal conditions of leaching at 79.99°C, acid concentration of 3.513/cm³, solid/liquid ratio of 0.021g/ml, stirring speed of 580.985rpm, particle size of 0.045mm, and reaction time of 240 minutes. This study amply demonstrates that the Box Wilson design is unquestionably a good method for examining the impact of significant process factors.

References

- [1] H.H. Murray, W.D. Keller. "Kaolins, kaolins, and kaolins" In: Murray, H.H., Bundy, W., Harvey, C. (Eds.), *Kaolin Genesis and Utilization*. The Clay Minerals Society, Boulder, CO, pp. 1–24, 1993.
- [2] S.U Ajana, O.D Onukwuli, R.O Ajemba, C.F Okey-Onyesolu, C.C Okoye, "Leaching of Okija kaolin iron-oxides impurity with HCl: optimization of dissolution conditions using Response Surface Methodology", *Integrated Journal of Engineering Research and Technology*, Vol 2 (3); 201-214, 2015.
- [3] I. A. Nnanwube, O.D Onukwuli, S.U Ajana, "Modeling and Optimization of Galena Dissolution in Hydrochloric Acid: Comparison of Central Composite Design and Artificial Neural Network". 294–315, 2018.
- [4] A. Martínez-Luévanos, M.G Rodríguez-Delgado, A. Uribe-Salas, F.R. Carrillo-Pedroza, J.G. Osuna-Alarcón. "Leaching kinetics of iron from low grade kaolin by oxalic acid solutions." *Applied Clay Science* 51, 473–477, 20 Jan. 2011. Web. 4 Aug. 2023.
- [5] F. Veglio, B. Passariello, L. Toro, A.M Marabini, "Development of a bleaching process for a kaolin of industrial interest by oxalic, ascorbic and sulphuric acids; preliminary study using statistical methods of experimental design." *Ind. Eng. Chem. Res.* 35, 1680–1687, 1996.
- [6] V.R. Ambikadevi, M. Lalithambika, "Effect of organic acids on ferric iron removal from iron-stained kaolinite." *Appl. Clay Sci.* 16, 133–145, 2000.
- [7] O.S Lee, T. Tran, Y.P Yi, S.J Kim, and M.J Kim. "Study on the kinetics of iron oxide leaching by oxalic acid." *International Journal of Mineral processing.* 80(2-4): 144-152, 2006.
- [8] S. Lee, T. Tran, B. Jung, S. Kim, M. Kim. "Dissolution of iron oxide using oxalic acid." *Hydrometallurgy* 87, 91–99, 2007.
- [9] M. Blesa, A. Marinovich, E. Baumgartner, A. Maroto. "Mechanism of dissolution of magnetite by oxalic acid-ferrous ion solutions". *Inorg. Chem.* 26, 3713–3717, 1987.
- [10] F. Veglio, L. Toro. "Factorial experiments for the development of kaolin bleaching process". *Int. J. Miner. Process.* 39, 87–99, 1993.
- [11] F. Veglio, L. Toro, "Process development of kaolin pressure bleaching using carbohydrates in acid media." *Int. J. Miner. Process.* 41, 239–255, 1994.
- [12] D. Panias, M. Taxiarchou, I. Douni, I. Paspaliaris, A. Kontopoulos. "Thermodynamic analysis of the reactions of iron oxides: dissolution in oxalic acid." *Can. Metall. Q.* 35, 363–373, 1996.
- [13] R. I Mitchell, Iriarte, B., Steinmetz, D., & Johnson, H. L. 1964, *Bol. Oobs. Tonantzintla Tacubaya*, 3, 153.
- [14] Y. Abali, M. Copur, and M. Yavuz, Determination of optimum conditions for dissolution of magnesite with H₂SO₄ solutions, *Indian Journal of Chemical Technology*, 13: 391-397, 2006.
- [15] W. Liu, M. Tang, C. Tang, J. He, S. Yang, J. Yang." Dissolution kinetics of copper ore in ammonia-ammonium chloride solution." *Transactions of Nonferrous Metals Society of China*, 20, 910 – 917, 2010.
- [16] M. Ozdemir, H Cetisli. Extraction kinetics of alumina in sulphuric acid and hydrochloric acid." *Hydrometallurgy*, 76(3-4), 217-224, 2005.
- [17] H. Poppleton, D. Sawyer. Hydrochloric Acid Leaching of Calcined Kaolin to Produce Alumina-Instruments and Experimental Techniques. English Translation of Pribory I. Tekhnika Eksperimenta, 2, 103-114, 1977.
- [18] J. Eisele, J. Bauer, D. Shanks. "Bench-Scale Studies to Recover Alumina from Clay by a Hydrochloric Acid Process." *Industrial & Engineering Chemistry, Product Research and Development*, 22(1), 105-110, 1983.
- [19] A. Al-Zahrani, M. H. Abdul-Majid, "Extraction of alumina from local clays by hydrochloric acid process. JKAU: Eng. Sci., 20(2), 27 – 39, 2009.
- [20] A. Kumar, B. Prasad, & I.M. Mishra. "Process parametric study of ethene carboxylic acid removal onto power activated carbon using Box-Behnken design." *Chem. Eng. Technol.*, 30(7), 932 – 937, 2007.
- [21] D. C. K. Ko, J.F. Porter, & G. Mckay. "Optimized correlations for the fixed bed adsorption of metal ions on bone char." *Chem. Eng. Sci.*, 55, 5819 – 5829, 2000.
- [22] K. Park, & J.H. Ahn, "Design of Experiment considering two-way interactions and its application to injection molding processes with numerical analysis." *Journal of Materials Processing Technology*, 146, 221 – 227, 2004.
- [23] A. Kumar, B. Prasad, & I.M. Mishra. Adsorptive removal of acrylonitrile using powered activated carbon. *Journal of Environmental Protection Science*, 2, 54 – 62, 2008.
- [24] G. Annadurai, R.S. Juang, & D.J. Lee. "Factorial design analysis of adsorption of activated carbon on activated carbon incorporated with calcium aginate." *Adv. Inorg. Environ. Res.*, 6, 191 – 198, 2002.
- [25] A. Shrivastava, P. Saudagar I. Bajaj, & R. Singhal, "Media optimization for the production of U-linolenic acid by *Cunninghamella echinulata* variegans MTCC 552 using response surface methodology." *International Journal of Food Engineering*, 4(2), 1-2, 2008.
- [26] Z. Alam, S.A. Muyibi, & N. Kamaldin. Production of activated carbon from oil Palm empty fruit bunches for removal of zinc. *Proceedings of Twelfth International Water Technology Conference, IWTC12 2008, Alexandria, Egypt*, 373-382, 2008.